THE JOURNAL OF BIOLOGICAL CHEMISTRY VOL. 285, NO. 2, pp. 1404–1413, January 8, 2010

Co-chaperone CHIP Stabilizes Aggregate-prone Malin, a Ubiquitin Ligase Mutated in Lafora Disease*[S]

Received for publication, April 13, 2009, and in revised form, November 4, 2009 Published, JBC Papers in Press, November 5, 2009, DOI 10.1074/jbc.M109.006312

Sudheendra N. R. Rao, Jaiprakash Sharma[1], Ranjan Maity, and Nihar Ranjan Jana[2]

From the Cellular and Molecular Neuroscience Laboratory, National Brain Research Centre, Manesar, Gurgaon-122 050, India

Lafora disease (LD) is an autosomal recessive neurodegenerative disorder caused by mutation in either the dual specificity phosphatase laforin or ubiquitin ligase malin. A pathological hallmark of LD is the accumulation of cytoplasmic polyglucosan inclusions commonly known as Lafora bodies in both neuronal and non-neuronal tissues. How mutations in these two proteins cause disease pathogenesis is not well understood. Malin interacts with laforin and recruits to aggresomes upon proteasome inhibition and was shown to degrade misfolded proteins. Here we report that malin is spontaneously misfolded and tends to be aggregated, degraded by proteasomes, and forms not only aggresomes but also other cytoplasmic and nuclear aggregates in all transfected cells upon proteasomal inhibition. Malin also interacts with Hsp70. Several disease-causing mutants of malin are comparatively more unstable than wild type and form aggregates in most transfected cells even without the inhibition of proteasome function. These cytoplasmic and nuclear aggregates are immunoreactive to ubiquitin and 20 S proteasome. Interestingly, progressive proteasomal dysfunction and cell death is also most frequently observed in the mutant malin-overexpressed cells compared with the wild-type counterpart. Finally, we demonstrate that the co-chaperone carboxyl terminus of the Hsc70-interacting protein (CHIP) stabilizes malin by modulating the activity of Hsp70. All together, our results suggest that malin is unstable, and the aggregate-prone protein and co-chaperone CHIP can modulate its stability.

Lafora disease (LD)[3] is a neurodegenerative epilepsy, characterized by progressively worsening seizure, myoclonus, dementia, and ataxia without any gender preference (1–3). The onset of the disease is typically between 12 and 17 years of age, and the patient usually dies within 10 years of the first seizure (1). One of the characteristic features of LD is the cytoplasmic accumulation of Lafora inclusion bodies containing polyglucosan in various organs including brain, liver, and axillary skin (4–6). Lafora bodies are ubiquitinated, suggesting that these inclusions also contain proteinaceous components (7).

It is an autosomal recessive disease caused by mutations in either of at least two genes *EPM2A* and *EPM2B* (8, 9). The *EPM2A* gene encodes laforin, a dual specificity phosphatase with a carbohydrate binding domain (10), and the *EPM2B* gene encodes malin, an E3 ubiquitin ligase of the ubiquitin proteasome system (UPS) (11). Patients with mutations in malin or laforin are phenotypically indistinguishable, and Lafora bodies are found across all LD patients (12). Current understanding suggests that both laforin and malin regulate glycogen metabolism, and therefore their loss of function might lead to the accumulation of Lafora bodies through deviant glycogen metabolism (13–17). How mutations in these two proteins induce neurodegeneration and whether Lafora bodies play any role in this process is not known.

The E3 ubiquitin ligase of the UPS plays a very important role in substrate recognition and exists with large diversity (18, 19). Because malin is an E3 ubiquitin ligase and its mutation causes LD, it is hypothesized that the improper degradation and accumulation of substrates of malin might lead to disease pathogenesis. Malin has been shown to promote proteasome-dependent degradation of laforin and glycogen debranching enzyme (amylo-1,6-glucosidase,4-α-glucanotransferase) (11, 15). Along with this, laforin-malin complex has been reported to efficiently degrade the protein targeting to glycogen, a regulatory subunit of protein phosphatase 1 as well as muscle glycogen synthase (17, 20).

Recently, malin and laforin have been demonstrated to be recruited to aggresomes upon inhibition of cellular proteasome function (21). Aggresome formation is a general response of cells, which occurs when the capacity of the proteasome is exceeded by the production of aggregation-prone misfolded proteins (22). Aggresomes are produced around the microtubule organizing center (MTOC), a subcellular structure involved in the degradation of cytoplasmic misfolded proteins (23). Aggresomes are also highly concentrated with various chaperones and components of UPS (23). The redistribution of malin to the aggresomes after proteasome inhibition suggested its probable involvement in the clearance of misfolded proteins (21). Subsequent studies from the same group have shown that the laforin-malin complex enhances the degradation of several misfolded mutant disease proteins including α-synuclein and expanded polyglutamine proteins (24). However, malin also forms aggregates, and several of its disease mutants show increased rates of aggregate formation in the absence or presence of proteasome inhibition. This suggests malin might be very prone to

* This work was supported by the Department of Biotechnology, Government of India.

[S] The on-line version of this article (available at http://www.jbc.org) contains supplemental Figs. S1 and S2.

[1] Supported by a research fellowship from the Department of Biotechnology, Government of India.

[2] To whom correspondence should be addressed. Tel.: 91-124-2338922; Fax: 91-124-2338910; E-mail: nihar@nbrc.ac.in.

[3] The abbreviations used are: LD, Lafora Disease; PBS, phosphate-buffered saline; DAPI, 4′,6-diamidino-2-phenylindole; FITC, fluorescein isothiocyanate; GAPDH, glyceraldehyde-3-phosphate dehydrogenase; UPS, ubiquitin proteasome system; MTOC, microtubule organizing center; GFP, green fluorescent protein; CHIP, carboxyl terminus of the Hsc70-interacting protein.

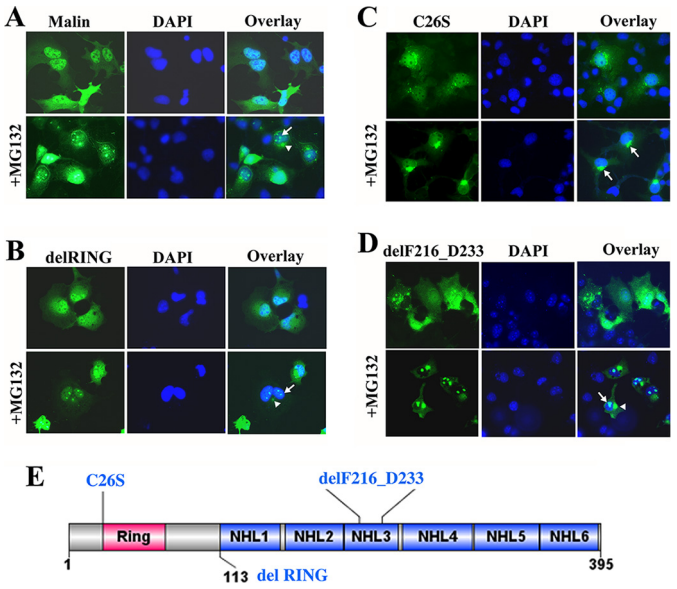

FIGURE 1. **Subcellular localization and aggregation of wild-type malin and its various LD-associated mutants in the presence and absence of proteasome inhibitor.** COS-7 cells were transiently transfected with plasmids (1 μg each/well of 2-well chamber slide) encoding wild-type malin, delRING malin, and two LD-associated mutants of malin (C26S and delF216_D233). Cells were left untreated or treated with MG132 (10 μM for 12 h), and at 24 h of post-transfection cells were processed for immunofluorescence staining. V5 antibody was used to detect wild-type (*A*) and delRING malin (*B*), Myc and FLAG antibodies were used to detect C26S (*C*), and delF216_D233 (*D*) mutants of malin, respectively. FITC-conjugated secondary antibody was used to stain and visualize the localization of malin and its mutants. DAPI was used to counterstain nuclei. *Arrowhead* indicates aggresomes, and the *arrow* shows nuclear aggregates of malin. *E*, schematic illustration on domain organization of malin and positions of various mutations that were used in the study.

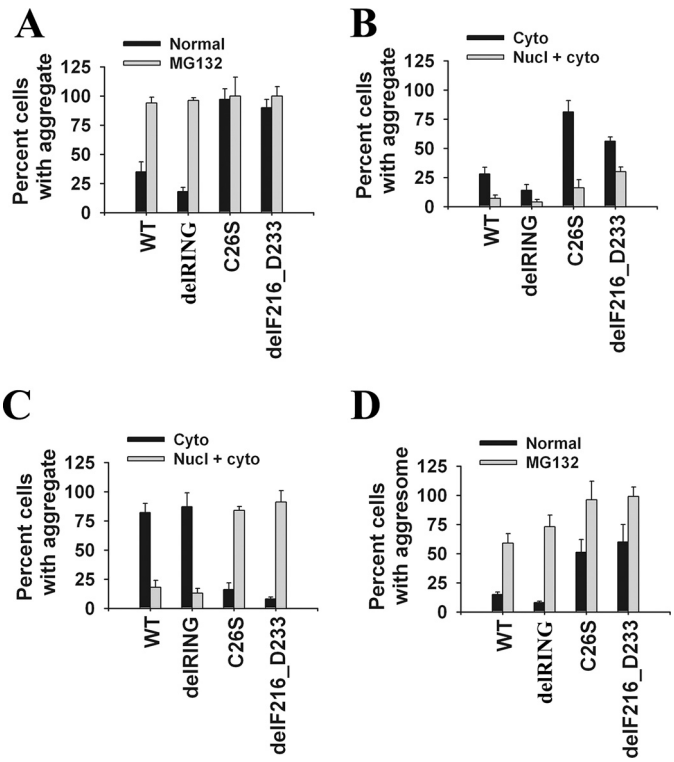

FIGURE 2. **Comparative analysis of the aggregation frequency among wild-type malin and its various mutants.** COS-7 cells were transiently transfected with wild type and various mutant constructs of malin and treated with MG132 in a similar way as was described in the legend to Fig. 1. Twenty-four hours after transfection, cells were subjected to immunofluorescence staining to visualize the localization and aggregation of malin and its mutants. Aggregates were counted in ~200 transfected cells for each plasmid. *A*, percentage of transfected cells forming aggregates in each plasmid transfected group in the absence and presence of MG132. In cells containing more than one, aggregates were considered to have single ones. Values are mean ± S.D. of three independent experiments. *B* and *C*, percentage of transfected cells having only cytoplasmic or cytoplasmic and nuclear aggregates in the absence (*B*) or presence (*C*) of MG132. Cells with only nuclear aggregates were rarely observed, and in most cases, nuclear aggregates accompany cytoplasmic aggregates. Values represent mean ± S.D. of three independent experiments. *D*, percentage of transfected cells forming aggresomes. Aggresomes were identified based on their juxtanuclear localization and co-localization with γ-tubulin (see supplemental Fig. S1). Values are mean ± S.D. of three independent experiments. *WT*, wild type; *Cyto*, cytoplasmic; *Nucl*, nuclear.

misfold, and various mutations have differential influence on its folding.

In this report, we demonstrate that overexpressed wild-type malin has a propensity to form aggregates, which increase dramatically after MG132 treatment. Expression of several mutants of malin also results in massive aggregation in both the cytoplasm and nucleus and induces progressive proteasomal dysfunction and cell death. Overexpressed malin associates with Hsp70, and its stability can be modulated by the co-chaperone CHIP.

EXPERIMENTAL PROCEDURES

Materials—The pcDNA3.1 V5/His TOPO TA cloning kit, Lipofectamine® 2000, optiMEM, and mouse monoclonal V5 antibody were purchased from Invitrogen. MG132, mouse monoclonal anti-FLAG, anti-γ-tubulin, and all cell culture reagents were from Sigma. Protein G-agarose, NBT, and BCIP were purchased from Roche Applied Science. The Bradford reagent was procured from Bio-Rad. Mouse monoclonal anti-Myc and anti-Hsp70, rabbit polyclonal anti-GAPDH, and anti-malin, goat polyclonal anti-CHIP, and anti-Hsc70 were purchased from Santa Cruz Biotechnologies. Hsp70 siRNA (a pool of 3 target-specific 20–25 nucleotide siRNA) along with control were purchased from Santa Cruz Biotechnologies. Rabbit polyclonal anti-ubiquitin and anti-20 S proteasome were procured from Dako and Calbiochem, respectively. Alkaline phosphatase- and fluorophore-conjugated secondary antibodies were purchased from Vector Laboratories.

Expression Plasmids—The full-length human malin was PCR amplified using genomic DNA extracted from SH-SY5Y cells and cloned into the pcDNA3.1 vector with a C-terminal V5 and His tags. The primer sequences were as follows: Forward, 5′-GCCATGGCGGCCGAA-3′; Reverse, 5′-CCCCCAGTCAAC-TTTATAGAC-3′. The NHL domain of malin (delRING malin) was also cloned into the same vector using the same reverse primer. The forward primer sequence was: 5′-GCCATGCTC-ACCTGCCACCACACC-3′. The source of human CHIP and delU box CHIP were described elsewhere (25). Mutant malin constructs (C26S and delF216-D233) were provided by Dr. S. Ganesh of IIT Kanpur, India. The plasmid pd1EGFP was purchased from BD Clontech.

Cell Culture and Transfection—COS-7, neuro 2a, and HEK293 cells were regularly maintained in Dulbecco's modified Eagle's medium with 10% fetal bovine serum and the antibiotics penicillin/streptomycin. Cells were equally plated into 6-well or 60-mm tissue culture plates at a subconfluent density and transfected after 24 h with Lipofectamine® 2000 according to

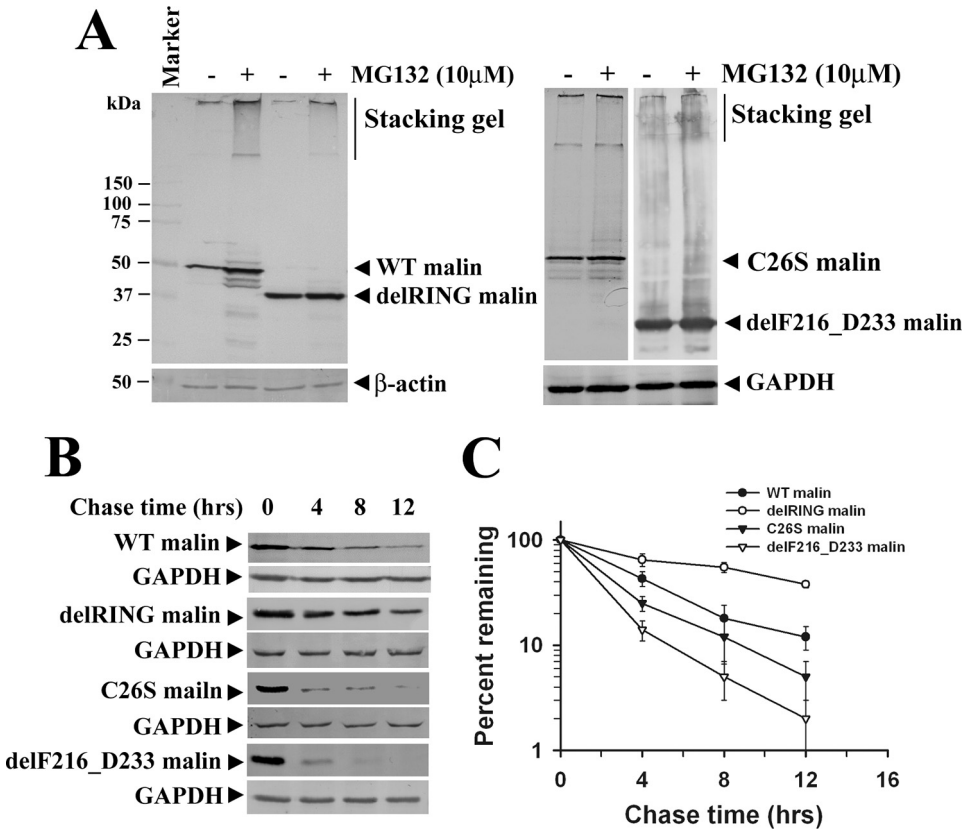

FIGURE 3. **Varying rate of degradation of malin and its several mutants through the proteasome.** *A*, wild type, delRING, and two LD-associated mutants of malin were transiently transfected into COS-7 cells (2 μg each/well of 6-well tissue culture plate) and treated with MG132 as described in the legend to Fig. 1. After 24 h of post-transfection, cells were collected and subjected to immunoblot analysis using V5 antibody (to detect wild-type and delRING malin), Myc antibody (to detect C26S malin) and FLAG antibody (to detect delF216_D233 deletion mutant of malin). *B*, cells were transfected with various malin constructs as described above. After 24 h of post-transfection, cells were treated with cycloheximide (20 μg/ml) and chased for different time periods indicated in the figure. Blots were probed with various antibodies to detect malin and its mutants. *C*, quantitation of the levels of malin and its mutants in the chase experiment described above. Quantitation was performed using NIH Image analysis software. Data were normalized against GAPDH. Values represent the mean ± S.D. of five independent experiments.

the manufacturer's instructions. For immunofluorescence staining, cells were plated into 2-well chamber slides. After 24 or 48 h of transfection, cells were used for immunofluorescence staining, co-immunoprecipitation, and immunoblotting.

Co-immunoprecipitation and Immunoblotting—Cells were collected 24-h post-transfection, washed in ice-cold PBS, pelleted by centrifugation, and lysed on ice for 30 min using Nonident P-40 (Nonidet P-40) lysis buffer (50 mM Tris, pH 8.0, 150 mM NaCl, 1% Nonidet P-40, complete EDTA-free protease inhibitor mixture). Cell lysates were collected after brief sonication and centrifugation at 20,000 × *g* for 20 min. Protein estimation was done using the Bradford method (26). Cell lysates were precleared with protein G-agarose beads. For each immunoprecipitation experiment, ~200 μg of protein in 0.2 ml of Nonidet P-40 lysis buffer were incubated with 2.5 μg of primary antibody. The total cell lysate or the immunoprecipitated proteins were separated through SDS-polyacrylamide gel electrophoresis and processed for immunoblotting as described elsewhere (25). Blots were scanned at 600 dpi and analyzed by Image J software (NIH) wherever applicable. All primary antibodies were used at 1:1000 dilutions except anti-V5 and anti-FLAG, which were used at 1:5000 dilutions.

Immunofluorescence Staining and Counting of Aggregates and Apoptotic Cells—COS-7 or neuro 2a cells grown in chamber slides were transiently transfected with appropriate plasmids. The treatment of MG132 (10 μM) and nocodazole (10 μg/ml) for 12 h was used when required. Cells were then washed in PBS and fixed with 4% paraformaldehyde in PBS for 30 min. After fixation, cells were washed again with PBS, permeabilized with 0.4% Triton X-100 in PBS for 10 min, and subsequently blocked with 5% nonfat milk in PBS or 3% bovine serum albumin for 1 h. Primary antibody incubation was carried out overnight at 4 °C. After several washes with PBS, cells were incubated with fluorophore-conjugated secondary antibody for 1 h. Cells were finally washed several times with PBS, mounted with DAPI, and imaged using the Axioplan fluorescence microscope/Apotome (Zeiss). Anti-V5, anti-Myc, and anti-FLAG were used at 1:1000 dilution; anti-CHIP, anti-Hsp70 at 1:200 dilutions; and anti-malin at 1:50 dilution.

Transfected Cells—Transfected cells showing apoptotic bodies and aggregates were typically counted at ×20 magnification. Fields were randomly chosen, and about 200–300 cells were counted per experiment. Each experiment was repeated at least three times, and counts were performed in a blinded manner.

Statistical Analysis—Statistical analysis was performed using SigmaStat software. Values are expressed as mean ± S.D. Intergroup comparisons were performed by two-tailed Student's *t* test. $p < 0.05$ was considered statistically significant.

RESULTS

Malin Is an Unstable, Aggregate-prone Protein, and Blockade of Proteasome Function Results in Its Massive Aggregation—To investigate the stability and aggregation-forming property of malin, we overexpressed human malin in COS-7, HEK293, and neuro 2a cells. 24 h later, cells were subjected to immunofluorescence staining with V5 antibody to detect malin. We observed that malin was localized both in the cytoplasm and nucleus with predominant nuclear staining. In the nucleus, malin was present in the nucleoplasm and apparently absent in the DAPI strong heterochromatin region (Fig. 1*A*). We often noticed aggregation of malin in the perinuclear and other cytoplasmic regions. The treatment of proteasome inhibitor MG132 dramatically increased the accumulation of malin

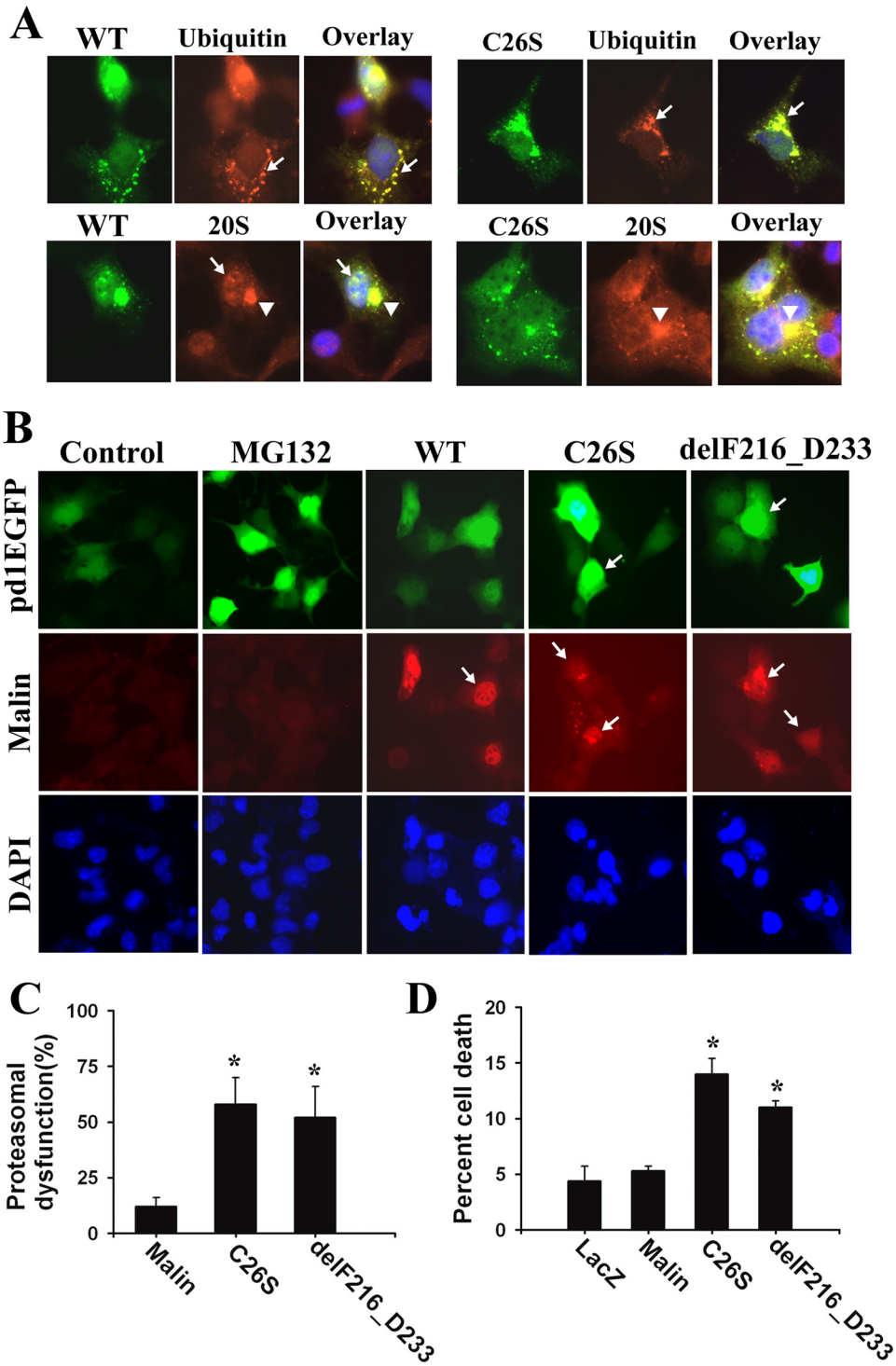

FIGURE 4. *A*, aggregates of malin or its mutants are co-localized with ubiquitin and the 20 S proteasome. Cells were plated into 2-well chamber slide and transfected with plasmids encoding wild type (*WT*) and C26S mutants of malin. 24 h later, cells were processed for dual immunofluorescence staining using either V5 and ubiquitin/20 S proteasome antibodies or Myc and ubiquitin/20 S proteasome antibodies. FITC-conjugated secondary antibody was used to label malin, and Texas Red-conjugated secondary antibody was used to detect either ubiquitin or the 20 S proteasome. The *arrow* indicates co-localization of ubiquitin and 20 S proteasome into aggregates produced by either wild type or C26S mutants of malin. The *arrowhead* shows localization of ubiquitin and 20 S proteasome into aggresomes. *B* and *C*, proteasomal dysfunction in the mutant malin-expressing cells. COS-7 cells were transiently transfected with various malin constructs (each 1 μg/well of 2-well chamber slide) along with pd1EGFP plasmid (500 ng/well). After 48 h of post-transfection, cells were subjected to immunofluorescence staining with V5, Myc, and FLAG antibodies to detect wild type, C26S, and delF216_D233 mutants of malin, respectively (*B*). The MG132-treated cells were used as a positive control, which showed a dramatic increase in the GFP fluorescence. *Arrow* indicates the malin-transfected cells showing proteasomal dysfunction. *C*, percentage of wild type or mutant malin-transfected cells exhibiting proteasomal dysfunction at day 3 as evaluated from the increased GFP fluorescence. Values are mean ± S.D. of three independent experiments with a minimum of 200 transfected cells scored for each experiment. *, $p < 0.01$ in comparison with wild-type malin-transfected cells. *D*, expression of LD-associated mutants of malin induces cell death. Percentages of transfected cells showing apoptotic features (fragmented nucleus, see supplemental Fig. S2) at day 3 were from three independent experiments. *, $p < 0.01$ in comparison with LacZ and wild-type malin-transfected groups.

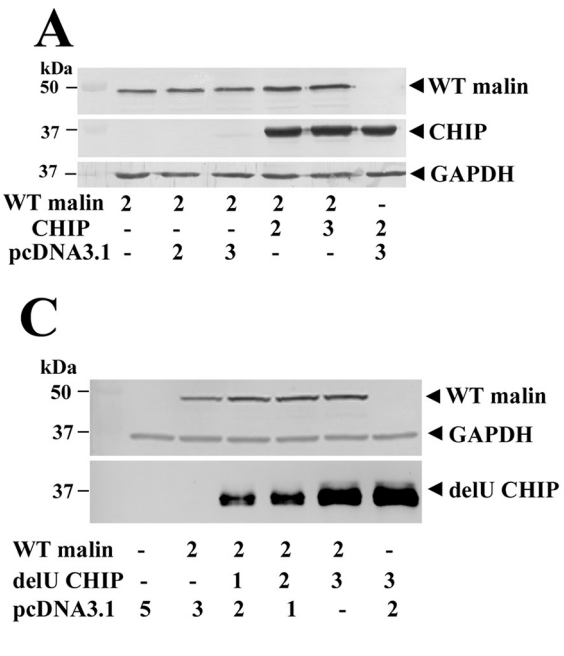

FIGURE 5. **Overexpression of CHIP- or its U-box-deleted construct increases the levels of malin.** COS-7 cells were co-transfected with plasmids encoding wild-type malin along with different concentrations of either CHIP (*A* and *B*) or delU CHIP (*C* and *D*) as indicated in the figure. Cells were collected 24 h post-transfection and subjected to immunoblot analysis with V5 antibody to detect malin and Myc antibody to identify either CHIP or delU CHIP. The band intensity of malin was quantified in cells that were transfected with equal amounts (2 μg of each plasmids) of malin and CHIP (*B*) or malin and delU CHIP (*D*). Data were normalized against GAPDH. Values are mean $\pm$ S.D. of three independent experiments. *, $p < 0.05$ in comparison with pcDNA3.1-transfected cells.

aggregates not only in perinuclear regions but also in other cytoplasmic areas and the nucleus (Fig. 1*A*). A similar subcellular distribution and aggregation profile in the absence and presence of MG132 was observed when the RING domain of malin was deleted (Fig. 1*B*). This finding indicates that the RING domain of malin had no influence on the nuclear localization as well as the aggregation-forming ability of malin. This pattern of subcellular localization and aggregation of malin was also consistent in neuro 2a and HEK293 cells (data not shown). Next we analyzed the subcellular distribution and aggregate formation of two mutants of malin reported in LD patients. The C26S mutation (missense) is located in the RING domain, whereas delF216_D233 (amino acid deletion) is in the 3rd NHL domain of malin. The localization patterns of both these mutant proteins were mostly similar to wild-type malin (Fig. 1, *C* and *D*). Interestingly, expression of these mutant proteins resulted in massive aggregation in the cell without the inhibition of proteasome function. Most of these mutant protein-expressing cells formed aggregates in cytoplasm and nucleus, and treatment of MG132 caused aggregation in 100% of the transfected cells (Fig. 1, *C* and *D*). Expression of these mutant constructs at very low levels (500 ng/well of 6-well tissue culture plate) for 24 h also caused aggregation in more than 50% of the transfected cells (data not shown). Approximately 2–5% of wild-type malin-transfected cells also formed aggregates under similar experimental conditions.

Next, we performed a detailed analysis and compared the aggregate formation among wild type and various mutants of malin (del RING, C26S, and delF216_D233). COS-7 cells were transfected with equal amounts of plasmids, and 24 h later, cells were processed for immunofluorescence staining to compare the aggregate formation. Approximately 40% of the wild-type malin-expressed cells showed aggregates that reached nearly 100% upon proteasome inhibition (Fig. 2*A*). Deletion of the RING domain of malin reduced the aggregation frequency. Expression of C26S or delF216_D233 mutants caused aggregation in about 100% of the transfected cells in the absence and presence of MG132 (Fig. 2*A*). However, MG132 treatment increased the number of aggregates in a single cell. Although wild-type or RING-deleted malins were predominantly nuclear, proteasomal inhibition did not produce many nuclear aggregates (Fig. 2, *B* and *C*). However, both disease mutants formed nuclear aggregates in more than 75% of the transfected cells upon proteasomal inhibition. Nuclear aggregates in any cells were always associated with cytoplasmic aggregates. The disease mutants of malin normally formed aggresomes in more than 50% of the transfected cells, which became 100% after MG132 treatment (Fig. 2*D*). Wild-type and RING-deleted malin exhibited aggresomes in more than 50% of the cells upon proteasome inhibition. Treatment of the microtubule-destabilizing agent nocodazole along with MG132 prevented aggresome formation but resulted in more numbers of aggregates throughout the cytoplasm (supplemental Fig. S1).

Because proteasomal dysfunction increased the aggregation of malin, we next analyzed the protein profile of malin and its several mutants in the absence and presence of MG132. As shown in Fig. 3*A*, the levels of wild type and various mutants of malin were increased in the presence of MG132. Accumulation of insoluble malin and its mutants were also detected in the stacking gel. Although the wild-type malin and several of its mutants were degraded by proteasome, cycloheximide chase experiments further revealed that they had varying rates of degradation (Fig. 3, *B* and *C*). The half-life of delF216_D233 and C26S mutants of malin were comparatively much shorter than wild-type malin. The deletion of the RING domain of malin further increased its half-life.

Expression of LD-associated Mutants of Malin Induces Progressive Proteasomal Dysfunction and Cell Death—We next checked the localization and redistribution of ubiquitin and proteasomes in the aggregates formed by malin or its various mutants. As expected, most of these aggregates (either cytoplasmic or nuclear) were ubiquitinated and associated with 20 S proteasome components (Fig. 4*A*). These findings further indicate that malin is targeted to proteasomal degradation. Protein aggregates in either the cytoplasm or nucleus is known to affect

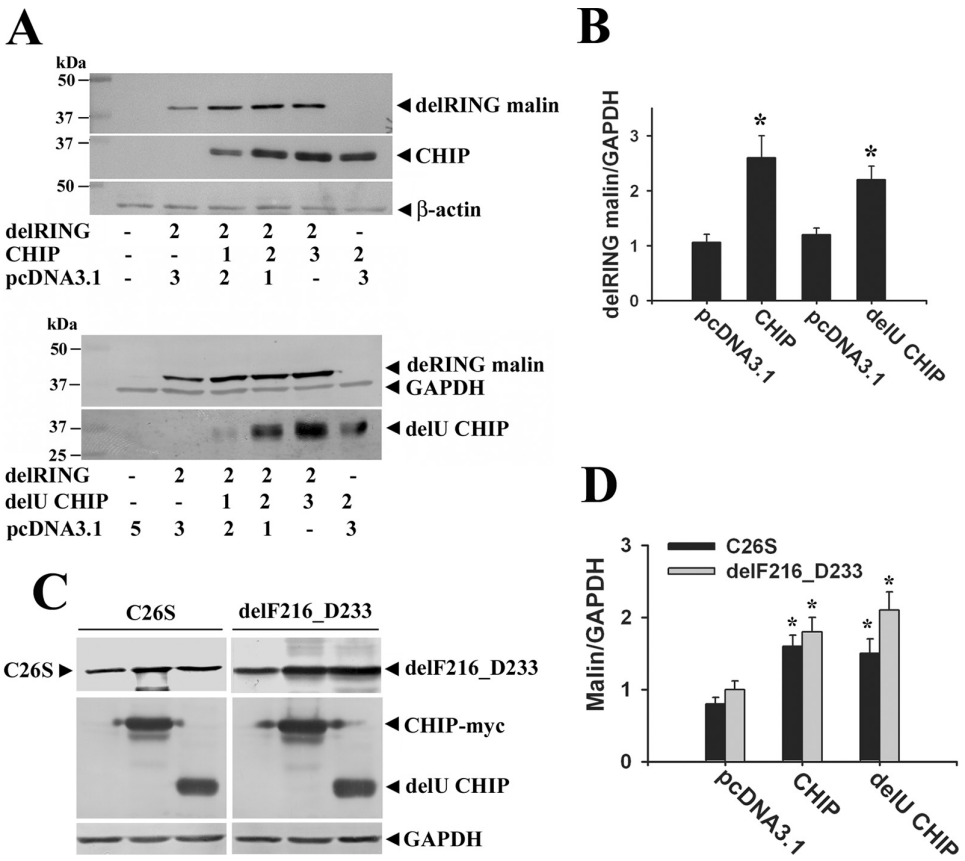

FIGURE 6. **Increased stability of various mutants of malin in the presence of CHIP.** Cells were transiently co-transfected with either delRING malin (*A* and *B*) or two LD-associated malin mutants (*C* and *D*) along with different or fixed concentrations of either CHIP or delU CHIP. 24 h after transfection, cells were collected and processed for immunoblot analysis with V5 (to detect delRING malin), FLAG (to detect delF216_D233 mutant of malin), and Myc (to identify C26S malin as well as CHIP and delU CHIP) antibodies. *B*, quantitation of the band intensity of delRING malin in cells that were transfected equal concentrations (2 μg of each plasmids) of either delRING malin + CHIP or delRING malin + delU CHIP plasmids. *D*, determination of the levels of mutant malins in the CHIP and delU CHIP-transfected cells. Plasmid concentrations were same as shown in *B*. Values are the mean ± S.D. of three independent experiments. *, $p < 0.05$ in comparison with pcDNA3.1-transfected cells.

the cellular proteasome function (27). Because several LD-associated mutants formed profuse aggregates, we further explored the effect of their expression on the cellular proteasome function. We have taken advantage of a model substrate of proteasome, which is a destabilized enhanced green fluorescence protein (d1EGFP) with a half-life of 1 h. This d1EGFP protein consists of multiple PEST (proline, glutamate, serine, and threonine) signal sequences at its C terminus that can be targeted for degradation by proteasome. The proteasomal dysfunction will increase the half-life of this protein and can be easily evaluated with increased fluorescence of GFP. The cells were transfected with wild type or mutants of malin along with the pd1EGFP plasmid for different time periods and then processed for immunofluorescence staining to detect malin. We then observed the fluorescence intensity of GFP in the various malin-transfected cells. As shown in Fig. 4*B*, expression of either C26S or delF216_D233 mutant of malin leads to impairment of cellular proteasome function as assessed from the increased GFP fluorescence intensity. About 20–30% and 50–60% of these mutant malin-transfected cells showed proteasomal dysfunction after 2 and 3 days of expression, respectively (Fig. 4*C*). Expression of wild-type malin also caused proteasomal dysfunction in about 10–15% transfected cells at day 3. Cells that expressed high levels of wild-type malin sometimes formed aggregates and generally demonstrated proteasomal malfunction. The MG132 was used as a positive control, and its exposure for 6 h produced massive proteasome impairment. The mutant malin-expressing cells also exhibited significant increases in apoptotic cell death (Fig. 4*D* and supplemental Fig. S2).

Co-chaperone CHIP Stabilizes Malin—We have observed that the deletion of the RING domain (responsible for ubiquitin ligase activity) of malin increased its half-life. This finding is consistent with a recent report that shows malin is auto-ubiquitinated and degraded by the proteasome (11). However, RING domain-deleted malin also degraded via proteasome, and amino acid deletion mutation of malin in the NHL domain also substantially decreased the half-life of malin. These observations clearly indicate that some other ubiquitin ligase is involved in the degradation of malin. We have explored the role of CHIP in the degradation of malin, because CHIP has been demonstrated to degrade misfolded proteins with the help of Hsp70/Hsc70 and function as a general cellular quality control ligase (28, 29). Different concentrations of CHIP plasmids were transfected along with wild-type constructs of malin for 24 h, and then the levels of malin were detected. To our surprise, overexpression of CHIP resulted in increased levels of malin in a concentration-dependent manner (Fig. 5, *A* and *B*). This effect of CHIP-induced stabilization of malin was unaffected upon deletion of the U-box domain of CHIP (Fig. 5, *C* and *D*). CHIP consists of an N-terminal TPR domain, which is responsible for interaction with Hsp70/Hsc70 and a C terminus U-box domain, involved in ubiquitin ligase activity. Our results indicate that the TPR domain of CHIP might be involved in the stabilization of malin. Next, we checked the effect of CHIP on the levels of RING domain-deleted malin as well as two LD-associated malin mutants. As shown in Fig. 6, overexpression of CHIP- or U-box domain-deleted CHIP also increased the levels of various mutants of malin. To explore the mechanism of CHIP-induced stabilization of malin, we first checked interaction of CHIP with malin. However, we failed to detect any possible co-immunoprecipitation of malin with CHIP (Fig. 7*A*). Under similar experimental conditions, CHIP was able to co-immunoprecipitate Hsp70 (Fig. 7*A*). Next we tested the interaction of malin with Hsp70 and found Hsp70 was co-immunoprecipitated with malin (Fig. 7*B*). To further confirm our findings, we

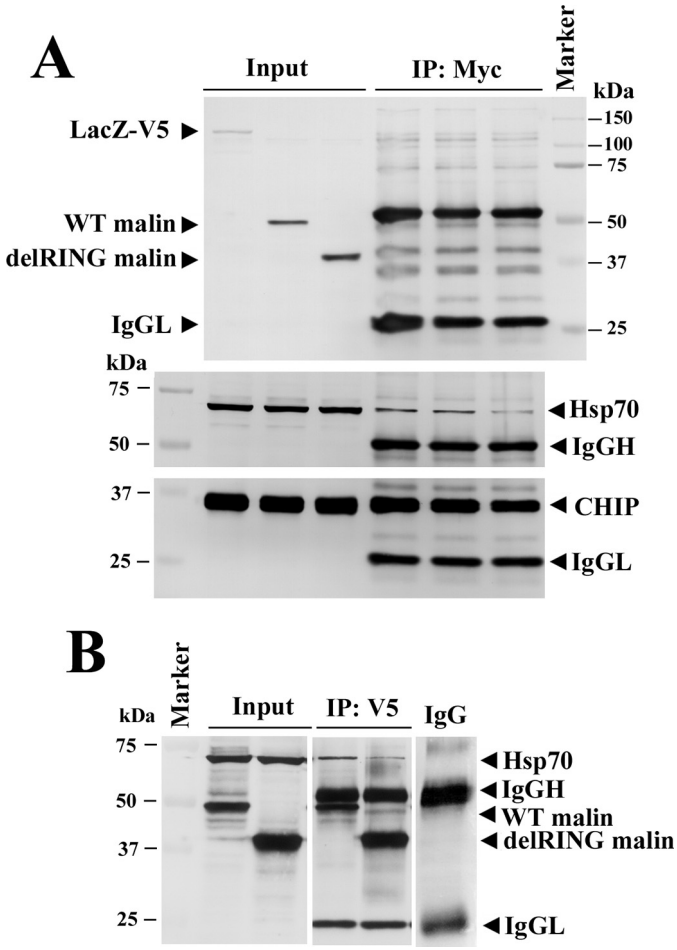

FIGURE 7. **Malin interacts with Hsp70 but not with CHIP.** *A*, COS-7 cells were co-transfected with plasmids encoding wild-type or delRING malin along with CHIP. Twenty-four hours after transfection, cells were collected; lysates were prepared, and then processed for co-immunoprecipitation using Myc antibody to pulldown CHIP. Blots were probed with anti-V5 (to detect wild-type and delRING malin), anti-Hsp70, and anti-Myc (to identify CHIP). CHIP was able to efficiently pulldown Hsp70 but not malin. *B*, wild-type or delRING malin plasmids were transfected into COS-7 cells for 24 h, and the cell lysates were subjected to co-immunoprecipitation with V5 antibody. Blots were probed with Hsp70 and V5 antibodies.

performed immunofluorescence co-localization study of CHIP and malin in COS-7 cells. As demonstrated in Fig. 8, CHIP was localized in the cytoplasm, whereas malin was predominantly in the nucleus. Malin was rarely co-localized with CHIP in the cytoplasm. CHIP was also never found to be associated with the aggregates of malin or its mutants (Fig. 8, *A* and *B*). But CHIP-overexpressed cells often exhibited increased levels of malin and its aggregation. Strikingly, overexpression of CHIP resulted in massive nuclear aggregation of mutant malin (Fig. 8*B*). The subcellular distribution of Hsp70 was very similar with malin and as expected, Hsp70 was co-localized with malin or its mutants and associated with their aggregates (Fig. 8*C*).

Our findings indicate that CHIP might be stabilizing malin through the modulation of Hsp70 function. CHIP is known to interact with the C terminus of Hsp70/Hsc70 and negatively regulates their chaperone activity. To confirm our hypothesis, we first tested the half-life of malin in the presence of CHIP. The overexpression of CHIP considerably increased (about 2-fold) the half-life of malin (Fig. 9, *A* and *B*). Next, we partially knocked down the Hsp70 and then checked the effect of CHIP on malin stabilization. As shown in Fig. 9*B*, partial knockdown of Hsp70 increased the levels of malin. Partial knockdown of Hsp70 also enhanced the CHIP-induced stabilization of malin.

DISCUSSION

Mutations in malin account for more than 50% of reported cases of LD (30, 31). Recently it was shown that malin and laforin recruited to aggresomes under proteasome impairment and the malin-laforin complex degrade misfolded proteins (21). Aggresomes are formed around the centrosome/MTOC, a subcellular region that is highly enriched with chaperones and components of UPS and is proposed to be involved in the degradation of cytoplasmic misfolded proteins (23, 32). Because malin is an ubiquitin ligase, its redistribution to MTOC was suggested to be the cells adaptive response to degrade misfolded proteins (21). Our findings suggest that malin-formed aggresomes might be because of its property to misfold spontaneously. Misfolded malin can be transported to centrosome/MTOC for proteasomal degradation, and inhibition of proteasome function could lead to its aggregation around centrosome/MTOC.

We have found that overexpressed human malin has the propensity to form aggregates, be degraded by proteasome, and form cytoplasmic and nuclear aggregates in almost all transfected cells upon proteasomal inhibition. Deletion of the RING domain of malin decreased the aggregate formation. More than 50% of the transfected cells form aggresomes as inferred by their juxta-nuclear accumulation and γ-tubulin staining. Destabilization of microtubular network using nocodazole under proteasome impairment prevented aggresome formation but results in profuse scattered aggregation all over the cytoplasm. Several disease-causing mutants of malin are very unstable having shorter half-lives and form aggregates in both the cytoplasm and nucleus in most transfected cells even without proteasomal inhibition. Their expression also results in progressive proteasomal dysfunction and cell death. Malin also interacts with Hsp70. Finally, the hydrophobicity profile generated using drawHCA (hydrophobic cluster analysis) at MOBYLE, a portal for bioinformatics analyses (a computer algorithm) and ProtScale at Expasy server, both suggested hydrophobic clusters in RING as well as NHL domains of malin (33–35). The computer-generated algorithm TANGO also predicted a very high aggregation-predisposed region in these domains (36). All these findings clearly suggest that the overexpressed malin is misfolded and targeted to MTOC for proteasomal degradation. Therefore, aggresomes of malin simply reflect cellular indigestion and may not be the cells strategy to degrade misfolded proteins. However, malin in the presence of laforin can be stabilized through interaction, and the malin-laforin complex can promote degradation of misfolded proteins.

Our findings are very similar to Parkin, another RING domain containing the E3 ubiquitin ligase mutated in juvenile Parkinson disease (37, 38). Parkin was shown to be forming aggregates including aggresomes when overexpressed and under various kinds of stress including proteasome impairment (39, 40).

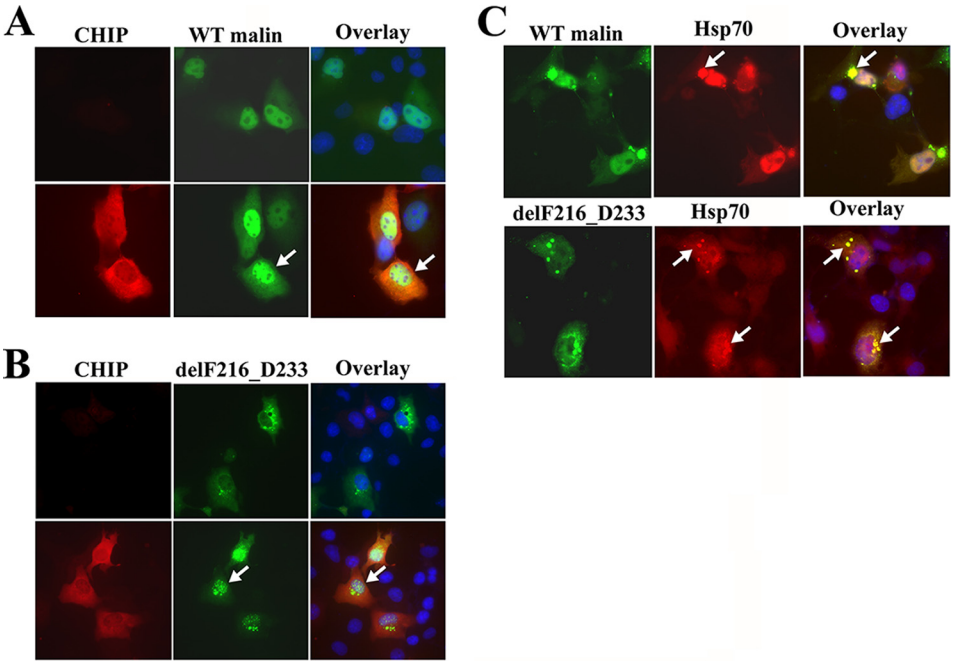

FIGURE 8. **Malin or its mutants co-localize with Hsp70 but not with CHIP.** *A* and *B*, COS-7 cells were co-transfected with plasmids encoding either wild type (*WT*) or delF216_D233 mutant of malin along with CHIP plasmid. Twenty-four hours of post-transfection, cells were used for double immunofluorescence staining with either CHIP and V5 antibodies or CHIP and FLAG antibodies. FITC-conjugated secondary antibody was used to localize wild-type or mutant malin and Texas Red-conjugated secondary was used to detect CHIP. The *arrow* indicates the increased level of wild-type malin or mutant malin aggregates in CHIP-overexpressed cells. *C*, COS-7 cells were transfected with either wild type or the delF216_D233 mutant of malin, 24 h later, cells were subjected to double immunofluorescence staining using antibodies against malin and Hsp70. FITC-conjugated secondary antibody was used to detect wild-type or mutant malin, and Texas-Red-conjugated secondary was used to localize Hsp70. The *arrow* indicates the localization of Hsp70 into aggregates produced by either wild type or delF216_D233 mutants of malin.

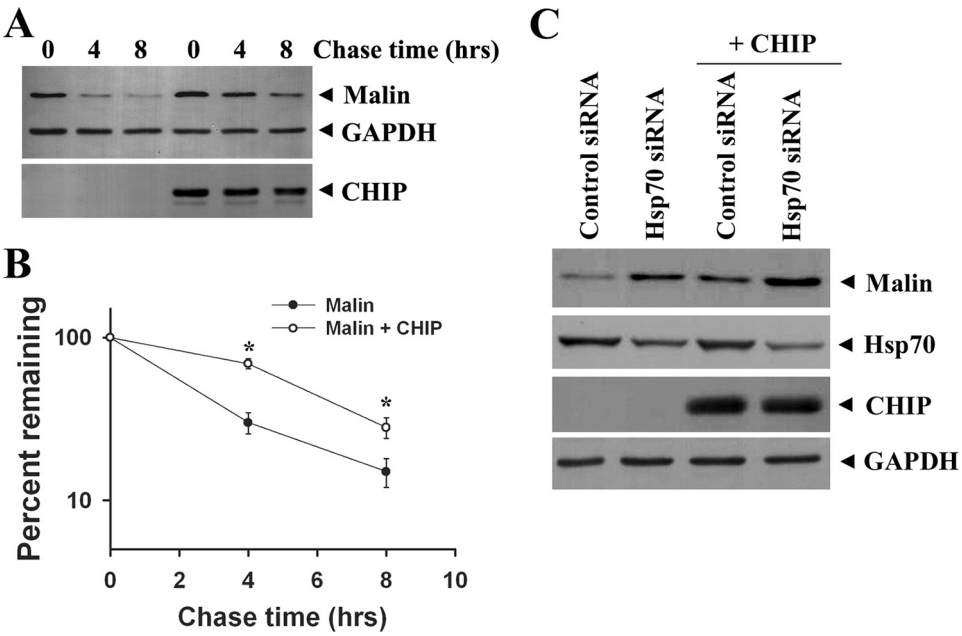

FIGURE 9. **CHIP-induced stabilization of malin requires Hsp70.** *A*, COS-7 cells were transfected with plasmids encoding malin and CHIP as descried in Fig. 5. Twenty-four hours later, cells were treated with cycloheximide (20 μg/ml) and chased for the different time periods shown in the figure. Blots were detected with antibodies against V5 (to identify malin), Myc (to detect CHIP), and GAPDH. *B*, quantitation of the levels of malin in the chase experiment described above from three independent experiments. Data were normalized against GAPDH. *, $p < 0.05$ in comparison with malin-transfected cells. *C*, cells were transfected with malin along with either control or Hsp70 siRNA (each 30 pmol/well of 6-well plate). In some experiments, CHIP was also co-transfected along with the above siRNA. Cells were collected at 48-h post-transfection and subjected to immunoblot analysis to identify malin, Hsp70, CHIP, and GAPDH.

Interestingly, most of the mutants of malin reported in LD exhibited increased propensity to form aggregates compared with the wild-type counterpart (21). Some mutants also show altered subcellular distribution, which has been proposed to be one of the causes underlying the disease pathogenesis. We have also observed a very high frequency of aggregate formation by two malin mutants (C26S and delF216_D233). However, their localization patterns are almost similar to the wild-type malin. They were predominantly localized in the nuclear compartment with weak punctate cytoplasmic staining. Most of the mutant malin (C26S and delF216_D233)-transfected cells showed cytoplasmic (50% were aggresomes) and nuclear aggregates when expressed at very low levels and without the inhibition of proteasome function. Almost all transfected cells showed aggresomes after proteasome impairment. Our findings along with others suggest that mutant malin might confer a toxic gain-of-function mechanism of disease pathogenesis similar to the many neurodegenerative disorders involving protein aggregation (41–43). Our findings of mutant malin-induced progressive proteasomal impairment and cell death further support this idea. In fact, very recently several mutants of laforin have been shown to induce cell death by an apparent gain-of-function mechanism (44). However, the mechanism of aggregation and the presence of mutant malin or laforin in Lafora bodies and proteasomal dysfunction in LD brain remain unknown and need further investigation.

We have also found that the wild-type malin is more stable in the nuclear compartment, because despite more than 50% of cells showing predominant nuclear localization, cytoplasmic aggregates were 7 times more common than nuclear aggregates. Within the nucleus, malin seems to be present in the nucleoplasm and conspicuously absent from DAPI-rich areas that

represent heterochromatin. Nuclear aggregates also co-localized with the 20 S proteasome. Interestingly in HepG2 cells, substrates of malin, namely laforin and glycogen-debranching enzyme have been shown to be transported to the nucleus under glycogenolytic conditions (15). However, glycogenolytic conditions have not been shown to influence subcellular localization of malin.

Malin levels are known to increase in the presence of its substrate laforin. This might be because of substrate-induced stabilization. In this context, surprisingly we found that CHIP can also act as a malin stabilizer. CHIP is known to interact with Hsp70/Hsc70 and negatively regulates their chaperone activity (45). CHIP also functions as a cellular quality control ubiquitin ligase and is known to degrade misfolded proteins with the help of chaperones Hsp70/Hsc70 (29, 46). Because both wild-type- and RING domain-deleted malin are misfolded and interact with Hsp70, we thought CHIP might be involved in the degradation of malin. To our surprise, we found that CHIP increased malin levels in a concentration-dependent manner, and maximum effect was found at a 1:1 ratio. The deletion of U-box domain of CHIP also increased the levels of malin, suggesting the involvement of the TPR domain in stabilization. Despite many repetitions (using triple detergent lysis buffer/Nonidet P-40 lysis buffer), we were unable to see any interaction between CHIP and malin. Immunofluorescence studies also did not reveal any possible co-localization of CHIP with malin and its aggregates. However, both malin and CHIP interacted with Hsp70. Interestingly, partial knockdown of Hsp70 increased the stability of malin, which can be amplified further upon overexpression of CHIP. CHIP is well known to interact with Hsp70/Hsc70 and negatively regulate their function (45, 46). Taken together, our findings indicate that the CHIP-induced stabilization of malin is probably mediated via the modulation of Hsp70 function. CHIP also has been shown to be associated with aggregate-prone Parkin and enhance its ligase activity (47). Whether CHIP can also increase the ligase activity of malin also needs to be explored.

In conclusion, we have shown that malin is an aggregate-prone cytoplasmic as well as nuclear protein. Malin is degraded by the proteasome, and inhibition of proteasome function results in its aggregation in both the cytoplasmic as well as nuclear compartment. Malin can be stabilized by the co-chaperone CHIP. Our findings also propose that toxic gain-of-function caused by malin mutations might account for part of the molecular basis of LD pathogenesis.

Acknowledgment—We thank Dr. S. Ganesh for providing mutant malin constructs.

REFERENCES

1. Minassian, B. A. (2001) *Pediatr. Neurol.* **25,** 21–29
2. Acharya, J. N., Satischandra, P., Asha, T., and Shankar, S. K. (1993) *Epilepsia* **34,** 476–487
3. Delgado-Escueta, A. V. (2007) *Curr. Neurol. Neurosci. Rep.* **7,** 428–433
4. Lafora, G., and Glueck, B. (1911) *Z. Zes. Neurol. Psychiatr.* **6,** 1–14
5. Nishimura, R. N., Ishak, K. G., Reddick, R., Porter, R., James, S., and Barranger, J. A. (1980) *Ann. Neurol.* **8,** 409–415
6. Carpenter, S., and Karpati, G. (1981) *Neurology* **31,** 1564–1568
7. Lohi, H., Ianzano, L., Zhao, X. C., Chan, E. M., Turnbull, J., Scherer, S. W., Ackerley, C. A., and Minassian, B. A. (2005) *Hum. Mol. Genet.* **14,** 2727–2736
8. Minassian, B. A., Lee, J. R., Herbrick, J. A., Huizenga, J., Soder, S., Mungall, A. J., Dunham, I., Gardner, R., Fong, C. Y., Carpenter, S., Jardim, L., Satishchandra, P., Andermann, E., Snead, O. C., 3rd, Lopes-Cendes, I., Tsui, L. C., Delgado-Escueta, A. V., Rouleau, G. A., and Scherer, S. W. (1998) *Nat. Genet.* **20,** 171–174
9. Chan, E. M., Young, E. J., Ianzano, L., Munteanu, I., Zhao, X., Christopoulos, C. C., Avanzini, G., Elia, M., Ackerley, C. A., Jovic, N. J., Bohlega, S., Andermann, E., Rouleau, G. A., Delgado-Escueta, A. V., Minassian, B. A., and Scherer, S. W. (2003) *Nat. Genet.* **35,** 125–127
10. Ganesh, S., Agarwala, K. L., Ueda, K., Akagi, T., Shoda, K., Usui, T., Hashikawa, T., Osada, H., Delgado-Escueta, A. V., and Yamakawa, K. (2000) *Hum. Mol. Genet.* **9,** 2251–2261
11. Gentry, M. S., Worby, C. A., and Dixon, J. E. (2005) *Proc. Natl. Acad. Sci. U.S.A.* **102,** 8501–8506
12. Singh, S., Sethi, I., Francheschetti, S., Riggio, C., Avanzini, G., Yamakawa, K., Delgado-Escueta, A. V., and Ganesh, S. (2006) *J. Med. Genet.* **43,** e48
13. Wang, W., Lohi, H., Skurat, A. V., DePaoli-Roach, A. A., Minassian, B. A., and Roach, P. J. (2007) *Arch. Biochem. Biophys.* **457,** 264–269
14. Solaz-Fuster, M. C., Gimeno-Alcañiz, J. V., Ros, S., Fernandez-Sanchez, M. E., Garcia-Fojeda, B., Criado Garcia, O., Vilchez, D., Dominguez, J., Garcia-Rocha, M., Sanchez-Piris, M., Aguado, C., Knecht, E., Serratosa, J., Guinovart, J. J., Sanz, P., and Rodriguez de Córdoba, S. (2008) *Hum. Mol. Genet.* **17,** 667–678
15. Cheng, A., Zhang, M., Gentry, M. S., Worby, C. A., Dixon, J. E., and Saltiel, A. R. (2007) *Genes Dev.* **21,** 2399–2409
16. Vernia, S., Solaz-Fuster, M. C., Gimeno-Alcañiz, J. V., Rubio, T., Garcia-Haro, L., Foretz, M., de Córdoba, S. R., and Sanz, P. (2009) *J. Biol. Chem.* **284,** 8247–8255
17. Worby, C. A., Gentry, M. S., and Dixon, J. E. (2008) *J. Biol. Chem.* **283,** 4069–4076
18. Glickman, M. H., and Ciechanover, A. (2002) *Physiol. Rev.* **82,** 373–428
19. Pickart, C. M. (2001) *Annu. Rev. Biochem.* **70,** 503–533
20. Vilchez, D., Ros, S., Cifuentes, D., Pujadas, L., Vallès, J., García-Fojeda, B., Criado-García, O., Fernández-Sánchez, E., Medraño-Fernández, I., Dominguez, J., García-Rocha, M., Soriano, E., Rodriguez de Córdoba, S., and Guinovart, J. J. (2007) *Nat. Neurosci.* **10,** 1407–1413
21. Mittal, S., Dubey, D., Yamakawa, K., and Ganesh, S. (2007) *Hum. Mol. Genet.* **16,** 753–762
22. Johnston, J. A., Ward, C. L., and Kopito, R. R. (1998) *J. Cell Biol.* **143,** 1883–1898
23. Kopito, R. R. (2000) *Trends Cell Biol.* **10,** 524–530
24. Garyali, P., Siwach, P., Singh, P. K., Puri, R., Mittal, S., Sengupta, S., Parihar, R., and Ganesh, S. (2009) *Hum. Mol. Genet.* **18,** 688–700
25. Jana, N. R., Dikshit, P., Goswami, A., Kotliarova, S., Murata, S., Tanaka, K., and Nukina, N. (2005) *J. Biol. Chem.* **280,** 11635–11640
26. Bradford, M. M. (1976) *Anal. Biochem.* **72,** 248–254
27. Bence, N. F., Sampat, R. M., and Kopito, R. R. (2001) *Science* **292,** 1552–1555
28. Murata, S., Minami, Y., Minami, M., Chiba, T., and Tanaka, K. (2001) *EMBO Rep.* **2,** 1133–1138
29. McDonough, H., and Patterson, C. (2003) *Cell Stress Chap.* **8,** 303–308
30. Singh, S., and Ganesh, S. (2009) *Hum. Mutat.* **30,** 715–723
31. Ianzano, L., Zhang, J., Chan, E. M., Zhao, X. C., Lohi, H., Scherer, S. W., and Minassian, B. A. (2005) *Hum. Mutat.* **26,** 397
32. Garcia-Mata, R., Gao, Y. S., and Sztul, E. (2002) *Traffic* **3,** 388–396
33. Wilkins, M. R., Gasteiger, E., Bairoch, A., Sanchez, J. C., Williams, K. L., Appel, R. D., and Hochstrasser, D. F. (1999) *Methods Mol. Biol.* **112,** 531–552
34. Callebaut, I., Labesse, G., Durand, P., Poupon, A., Canard, L., Chomilier, J., Henrissat, B., and Mornon, J. P. (1997) *Cell Mol. Life Sci.* **53,** 621–645
35. Neron, B., Menager, H., Maufrais, C., Joly, N., Tuffery, P., and Letondal, C. (2008) *Mobyle: a New Full Web Bioinformatics Framework*, Bio Open Source Conference (BOSC), Toronto
36. Fernandez-Escamilla, A. M., Rousseau, F., Schymkowitz, J., and Serrano, L. (2004) *Nat. Biotechnol.* **22,** 1302–1306

37. Kitada, T., Asakawa, S., Hattori, N., Matsumine, H., Yamamura, Y., Minoshima, S., Yokochi, M., Mizuno, Y., and Shimizu, N. (1998) *Nature* **392,** 605–608
38. Shimura, H., Hattori, N., Kubo, S., Mizuno, Y., Asakawa, S., Minoshima, S., Shimizu, N., Iwai, K., Chiba, T., Tanaka, K., and Suzuki, T. (2000) *Nat. Genet.* **25,** 302–305
39. Junn, E., Lee, S. S., Suhr, U. T., and Mouradian, M. M. (2002) *J. Biol. Chem.* **277,** 47870–47877
40. Ardley, H. C., Scott, G. B., Rose, S. A., Tan, N. G., Markham, A. F., and Robinson, P. A. (2003) *Mol. Biol. Cell* **14,** 4541–4556
41. Taylor, J. P., Hardy, J., and Fischbeck, K. H. (2002) *Science* **296,** 1991–1995
42. Muchowski, P. J., and Wacker, J. L. (2005) *Nat. Rev. Neurosci.* **6,** 11–22
43. Lansbury, P. T., and Lashuel, H. A. (2006) *Nature* **443,** 774–779
44. Liu, Y., Wang, Y., Wu, C., Liu, Y., and Zheng, P. (2009) *Hum. Mol. Genet.* **18,** 2622–2631
45. Ballinger, C. A., Connell, P., Wu, Y., Hu, Z., Thompson, L. J., Yin, L. Y., and Patterson, C. (1999) *Mol. Cell. Biol.* **19,** 4535–4545
46. Murata, S., Chiba, T., and Tanaka, K. (2003) *Int. J. Biochem. Cell Biol.* **35,** 572–578
47. Imai, Y., Soda, M., Hatakeyama, S., Akagi, T., Hashikawa, T., Nakayama, K. I., and Takahashi, R. (2002) *Mol. Cell* **10,** 55–67